NordFou: External Influences on Spray Patterns (EPAS)

Report 13: Experimental determination of key parameters for the Salt Spreading Simulation Software 3-S

Hisamitsu Takai[1], Torben Brøchner[2] and Jan S. Strøm[1]

1) Aarhus University, Dept. of Engineering, Engineering Centre Bygholm, Schüttesvej 17, Building 67-04, 8700 Horsens, Denmark

2) VIA University College, Centre for Applied Research and Development in Building, Energy & Environment, Chr. M. Østergaards Vej 4, 8700 Horsens, Denmark

Abstract

A Salt Spreading Simulation (3-S) software is currently under development at the Engineering Centre Bygholm (ECB). The aim of the software is to simulate motion of salt particles that are spread by a spinning spreader disk, flying under the influence of gravity and wind, bouncing on the road surface and finally be positioned on the road in a spreading pattern.

The aim of this experimental study was to determine some key parameters for the software. The materials studied were particle samples of dry rock salt and vacuum salt. The present report covers three partial studies: "Visual observation of particle motion", "Shape and mass of particles" and "Bouncing behaviour on different materials".

Visual observation of salt particle motion by high speed camera turned out to be a feasible way to get an overview. However, the resolution of 224×56 pixels for the frame rate of 1000 fps was not sufficient to obtain a sharp image of a particle moving with a velocity of about 6 m s^{-1}. Halogen and fluorescent lamps turned out to be good light sources. Even for a small laboratory setup it was found that four lamps with the total effect of more than 2000 W was required to get an acceptable light intensity for recording of high speed movies.

The largest particle fraction (32%) of rock salt was found in the size interval 2.8-4.0mm. The average particle masses were found to be 0.3 mg $particle^{-1}$ in the size interval 0.5 to 1mm, 2 mg $particle^{-1}$ for 1-2mm, 10 mg $particle^{-1}$ for 2-2.8mm, 28 mg $particle^{-1}$ for 2.8-4mm and finally 65 mg $particle^{-1}$ for particles > 4mm. It was found that the average mass of salt particles in the size intervals can be estimated by the mass of equivalent spherical particles. Furthermore, particles dropped freely onto a polished horizontal surface of stainless steel bounced evenly to all directions. These observations lead to a conclusion that the rock salt particles can be considered as objects with random shape characteristics.

Bouncing behaviour was studied for particles with masses from 10 to 100 mg. They achieved an impact velocity of around 3 m s^{-1} when they were dropped from a height of 0.4m. With this impact velocity it was observed that a thin water layer on the surface reduced the particle bouncing. However, this phenomenon was highly influenced by the kinetic energy of the particle meaning that large particles was not so much affected by the water layer. Furthermore, particles impacting the surface with a low angle, i.e. approx.15^{o}, and with a velocity of 6 m s^{-1}, did not bounce backward. Also, it was observed that even polished surfaces can cause spinning of

particles. Finally, it was seen that salt particles (vacuum salt) tend to be sticking to the surface after the impact.

Introduction

A Salt Spreading Simulation (3-S) software is currently under development at the Engineering Centre Bygholm (ECB). The aim of the software is to simulate motion of salt particles that are spread by a spinning spreader disk, flying under the influence of gravity and wind, bouncing on the road surface and finally be positioned on the road in a spreading pattern.

The software is still at its first development stage, where a number of assumptions and parameters are introduced without ensuring appropriate information about their consistency. The aim of this experimental study was to determine some key parameters for the software. The materials studied were samples of dry rock salt and vacuum salt. The present report covers three partial studies: 1) “Visual observation of salt particle motion”, 2) “Shape and mass of rock salt particles” and 3) “Bouncing behaviour of salt particles on different materials”.

Visual observation of salt particle motion”

As this partial study dealt with detailed observation of small particles, two contradictory requirements had to be considered: It is desired to obtain a wide view angle and at the same time to benefit from high-resolution. A high speed camera that fulfilled these criteria was therefore desirable.

Furthermore, the light level for observing moving salt particles must be high enough to capture images with very short exposure time. Besides, the diaphragm opening for such a camera must be small to obtain a proper depth of field to ensure sharp images of the particles. Some high speed cameras for professional use might fulfil these requirements fully or partly. But, their prices were too high for the project budget. In the recent years, more affordable high speed movie cameras and high light sensitive cameras for non-professional users were introduced in the market. The present study used such cameras.

The salt particle motion was captured using a Casio high speed movie camera type Exilim EX-FH20. It is an easy to use camera. The particle motion was analysed using the video editor Avidemux 2.5.4 (http://fixounet.free.fr/avidemux/).

In some situations a Sony camera type NEX-5R was used due to its superior light sensitivity. A red laser sheet was used to recognize white salt particle because salt surfaces reflect laser light clearly enough to be recorded on a movie film.

The major technical specifications for these two cameras are shown in Table 1 and 2.

Halogen lamps turned out to be good light sources for observation of moving salt particles. To illuminate the spreading patterns behind a salt spreading disc three 500-W and one 1000 W halogen lamps were used for movements over longer distances for 210 fps-movies as shown in figure 1A.

To illuminate the small area, where particle motion was studied, two 500 W and one 1000 W halogen lamps plus one 100 W fluorescent lamp was used over smaller distances for 420 fps-movies as shown in Figure 1B.

Light intensity was often not enough to take a good high-speed movie; but acceptable for simple analysis. Other light sources, like high intensity discharge lamps or mercury quartz lamp may be used as alternatives. However, the natural light intensity from the sun is much higher. So, recording of high-speed movies in open air or inside a greenhouse are alternatives that are likely to be used in relation to future salt spreading experiments.

A blue and a red laser sheet were tested with focus on its ability to enhance the recognition of white salt particles. The red DeWalt laser type DW087K turned out to be superior and was used for this purpose.

The experience is that a light sensitive high speed camera with a frame rate up to 1000 fps are useable for recording of salt particle motions. For illumination of indoor experiments halogen lamps or fluorescent lamp can be used. However, whenever possible natural sun light should be used. The red laser was useful to enhance the recognition of white salt particles because it reflects clear light to the camera.

Table 1: Major technical specifications of Casio Exilim EX-FH20

Focal point distance		**4.6 – 92 mm**
Lens, f-number		2.8 (W) – 4.5 (T)
ISO sensitivity		100 – 1600
Effective sensor resolution		9.14 mega pixels
Min. camera-to-subject distance		Ca.1 cm (Still image) Ca.12 cm (movie)
Zoom		20 times (Optical), 4 times (Desital)
Continuous shooting speed (fps)		3, 5, 10, 15, 30 and 40
Recording mode	Still image	RAW(DNG), JPEG, DCF; DPOF
	Movie	AVI, Motion JPEG, IMA-ADPCM
Movie; Frame rate, frames per sec (fps.)		Image size
30 (Standard)		640 x 480 pixels
30 (HD)		1280 x 720 pixels
210		480 x 360 pixels
420		224 x 168 pixels
1000		224 x 56 pixels

Table 2: Major technical specifications of Sony NEX-5R

Camera type		Interchangeable lens, E-mount lens
Focal point distance		2.7 – 82,5 mm
Lens, f-number		3,5 (18mm) – 5,6(55mm)
ISO sensitivity		Still image: 100 – 25600; Movie: 100 - 6400
Effective sensor resolution		16,1 mega pixels
Min. camera-to-subject distance		25 cm
Continuous shooting speed (fps)		Normal: 3 fps, Max: 10 fps
Recording mode	Still image	JPEG, RAW, DPOF
	Movie	AVCHD/MP4, MPEG-4 AVC(H264)
Movie; Frame rate, frames per sec (fps.) and recording mode		Image size
30 (AVCHD)		1920 x 1080 pixels
30 (AVC MP4)		1440 x 1080 pixels
	VGA	640 x 480 pixels
30 (MPEG4 MP4)		1280 x 720 pixels
	VGA	640 x 480 pixels

A Longer distances

B Short distances

Figure 1: A high light intensity was required for taking a high speed movie of salt particles.

Shape and mass of rock salt particles

The shape of rock salt particles is assumed to be perfectly random so they can be considered as spherical in average. Thus, the first step for validation of the assumption is to explore the randomness of the shape of rock salt particles. Two different experimental methods were explored for the purpose.

The first experiment was to compare the experimentally derived curve for particle size and mass relationships with the curve derived from the calculated mass of ideal spherical salt particles. The comparison gave an indication of the shape randomness of the particles. Perfectly randomly shaped particles should produce same curve as the calculated curve when the number of particles are sufficiently large. Thus, the deviation of these two curves indicates the level of randomness.

The second experiment was to let a large number of particles fall down onto a horizontal flat surface and observe the distribution of settled particles. The locations where particles settle on the surface after the impact, bouncing and rolling should reflect the shape of the particles. If the particles are perfectly random shaped they should be distributed evenly in all directions. Thus such deviation indicates the shape randomness.

An example of the variation in the shape and size of rock salt particles are shown in Figure 2. If the shapes of particles are perfectly random the average shape might be spherical. Thus, simulating motion of spherical salt particles would be a feasible way to estimate the average trajectory of the salt particles.

Size and mass distribution of rock salt was analysed by a standard set of laboratory test sieves (ASTME 323, Endecotts LTD, London) with size intervals < 0.5, 0.5 to 1, 1 to 2, 2 to 2.8 to 4 and > 4mm. The result is shown in Figure 3. The largest fraction by weight was found on 2.8 – 4.0 mm sieve with 32% of the total sample mass.

The mass of a single salt particle was determined with a laboratory balance. A particle in the smallest size interval under 0.5mm was below the detection limit for the method applied. It was not possible to isolate the influence of humidity on very small salt particles.

Figure 4 shows the average particle mass in the size intervals from 0.5mm and up were 0.3, 2, 10, 28 and respectively 65 mg particle^{-1} and the calculated mass of spherical salt particles using the lowest limit of the size intervals. The correspondence between the two curves indicates that a reliable prediction of an average mass of salt particles in a size interval is possible. It also indicates that the 3D-shape of particles is random so that their "average" shape can be considered to be spherical.

Figure 2: Size and shape variation of rock salt particles.

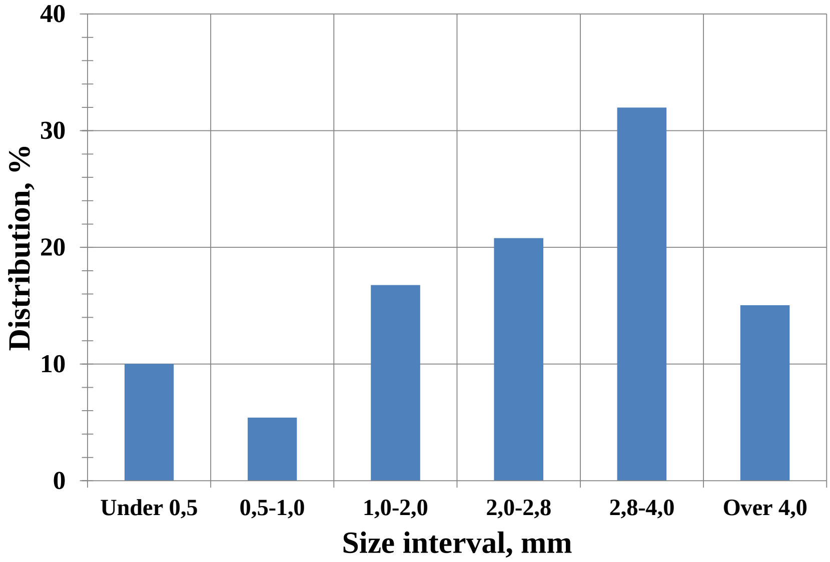

Figure 3: Mass distribution for six size intervals for the sample of rock salt.

Figure 5 shows the free-fall bouncing test setup. Large salt particles (> 2.8 mm fractions) were used. Particles fell from a plate placed 0.4 m above the horizontal surface of a polished stainless steel plate. About 500 salt particles were carefully pushed one by one over the edge of an opening (ø 30mm) in a Plexiglas (acrylic plastic) panel. If the salt particles are randomly shaped, they will bounce and settle in random directions after a vertical fall.

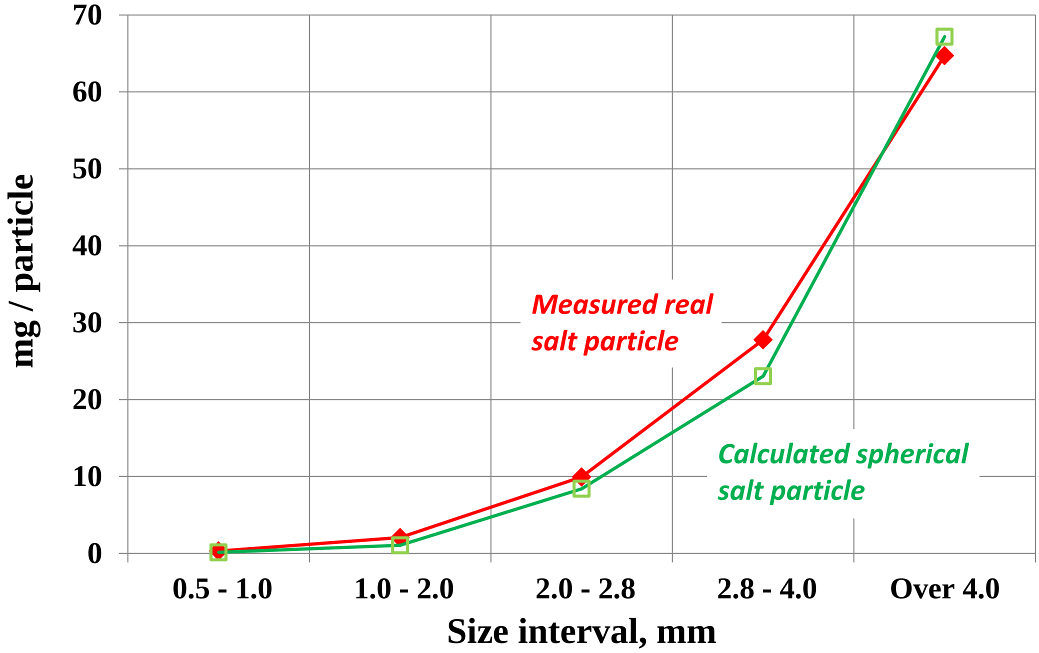

Figure 4: Comparison between measured average mass of a real salt particles and the calculated mass of spherical salt particles.

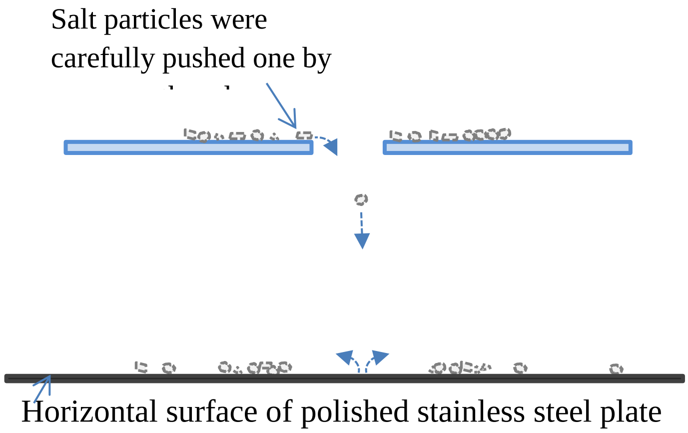

Figure 5: Sketch of the setup for bouncing test.

Figure 6 shows the result of a bouncing test. Salt particles seem to be distributed evenly in all directions, indicating that the salt particles were randomly shaped.

The observations lead to the conclusion that rock salt particles taken as a whole can be considered as deviations from a perfect sphere. This “shape randomness” means that salt particles are going to be implemented as perfect spheres in the deterministic approach of the 3-S software.

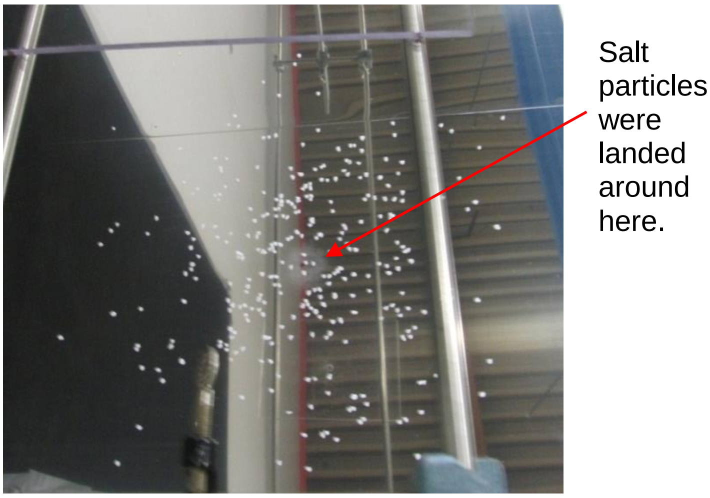

Figure 6: Distribution of salt particles after bouncing on a horizontal stainless steel plate.

Bouncing behavior of salt particles on different materials

When the salt particles are impacting the road surface it is observed that the particles combine jumping, sliding and rolling. All of these three impact types are further dependent on the irregular geometry of both the salt particles and the road surface. The chemical/mechanical interactions between salt, additives, snow, ice, water, and the road friction are complicated. Visual observation and analyses of slow motion video replay may give an overview of the phenomenon and ideas about the importance of the parameters, e.g. impact angle and velocity, surface condition, mass, shape of particles and probably more.

The objective of this experiment series was to get an overview of the motions of salt particles at impact with the road surface and to identify the study directions.

The study included two separate experiments: 1) Free fall vertical impact and 2) High speed low angle impact. For both experiments dry and wet roofing felt was used to simulate real road surfaces. The wet surface was prepared by letting an amount of water float over the surface until the surface was completely covered by a thin water layer.

A sketch and a photo of the experimental setup used to study free-fall impact are shown in Figure 7. Salt particles of known mass from 10 to 100 mg were placed one-by-one in the holes of the slider. Then they fall singly through the opening in the guide-plate as they were pushed to the opening by the slider. The motions of particles bouncing on the surfaces were captured by the high speed camera with a frame rate of 420 fps, see Figure 8.

A special experimental device, the “salt canon” Figure 9, was designed to create high speed low angle impact with the surface. It was constructed to simulate the ejection of a salt particle from a spreading disc.

A small portion of particles was fed through an opening in the pipe wall, while a spring loaded iron bar was kept in pulled position by a trigger. It could shoot salt particles with initial velocities of up to about 6 m s^{-1}, depending on the mass of the particles and the spring tension.

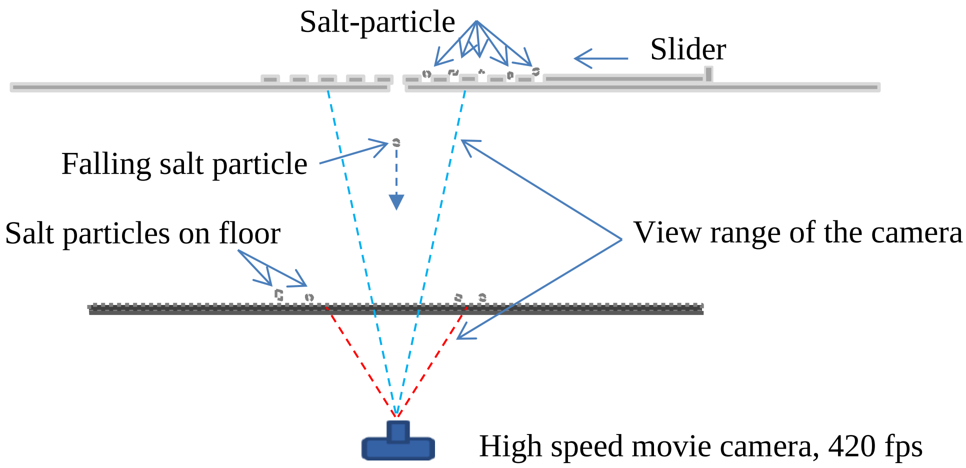

Figure 7: Sketch of the free-fall test

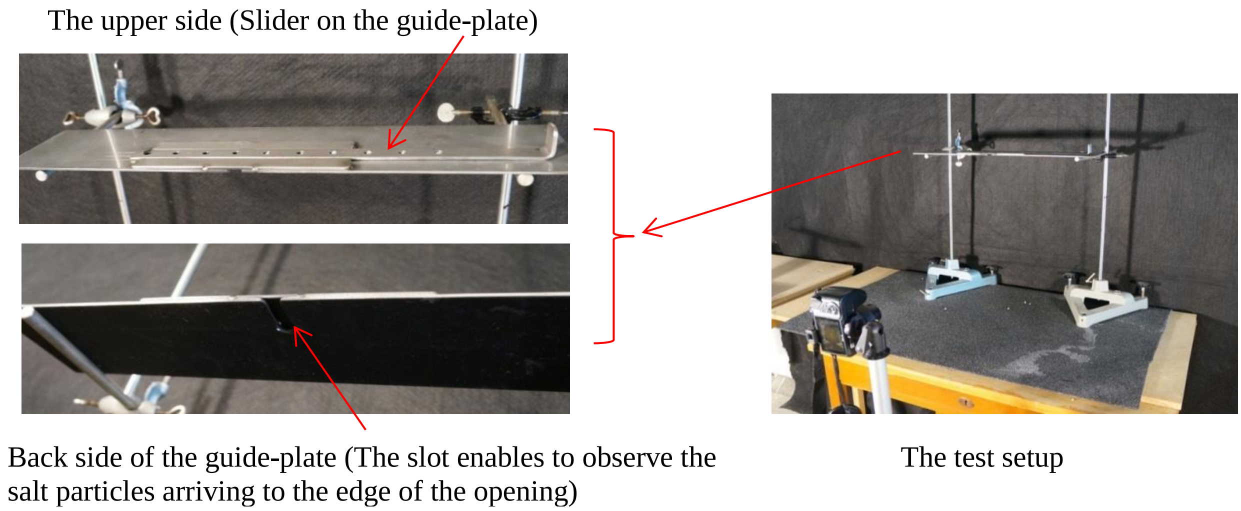

Figure 8: Photos of the free fall test setup

White salt particle reflects red laser light clearly enough to be recognized in the movie film. A red laser sheet generator was placed at a extend distance from the top edge of the salt canon. The time of flight can be determined by analysing number of frames between the moment when the salt particles are visible at the top edge of the salt canon and the moment when the salt-swarm-front passing through the red laser sheet. Then the average velocity over the distance can be determined, Figure 10.

Small portions, ca. 3 g, of large salt particles (> 2.8 mm) and small salt particles (vacuum salt) were shot against the surfaces. Particle motions were captured with a frame rate of 210 fps.

Particles ejected by the salt canon impacted the surface with an average velocity of about 6 m s^{-1} and the landing angle was about 15°. The landing angle is comparable to the angle when salt particles are spread horizontally with an initial velocity of 10 m s^{-1} from a spreader disc placed 0.4m above the road surface (Takai, 2012a and Takai, 2012b). The velocity of the particles spread from a moving truck is sum of two velocity vectors, i.e. the velocity created by the spreader and the velocity of the truck. And, the large particles are expected to maintain the velocity during the

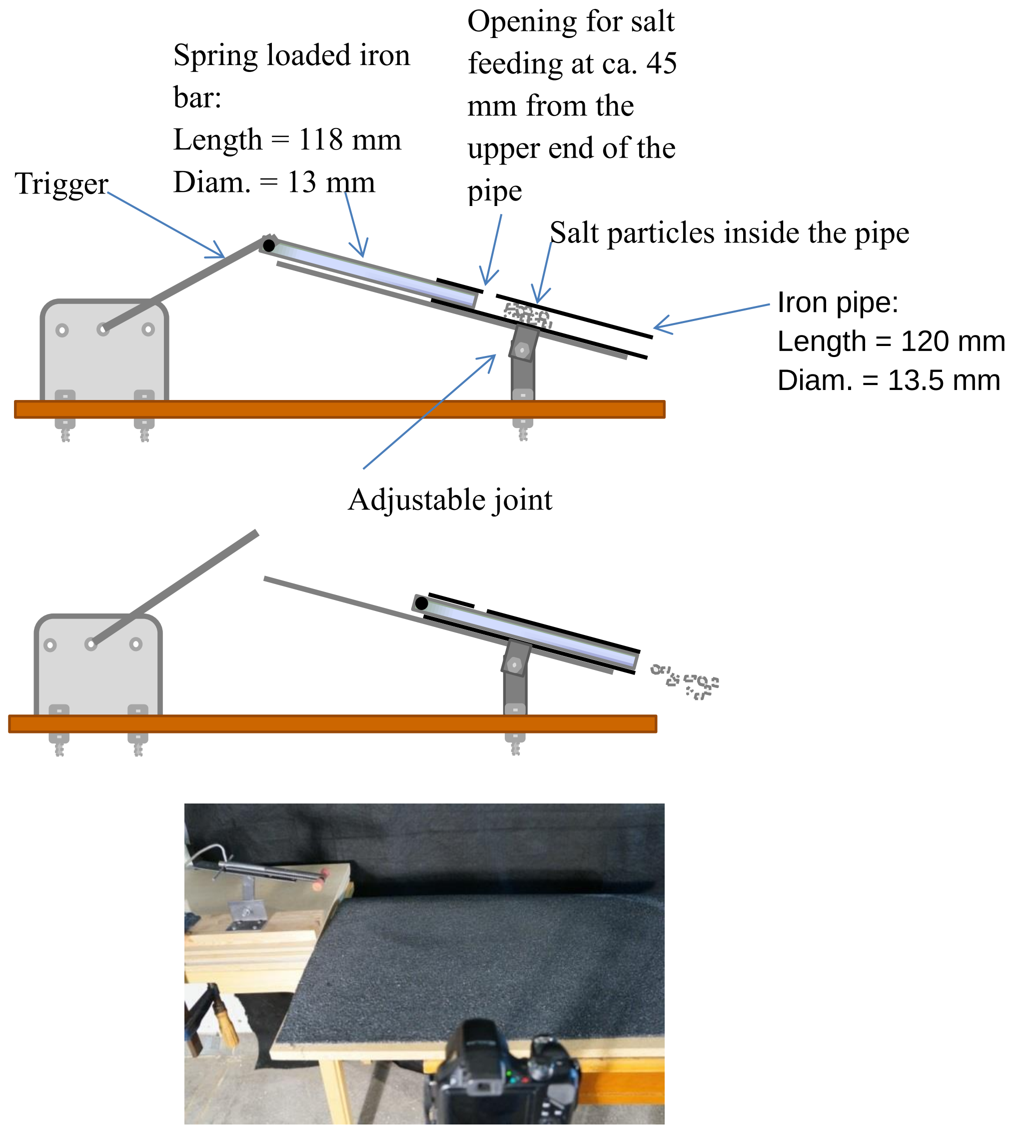

Figure 9: Sketch and photo of the salt canon setup.

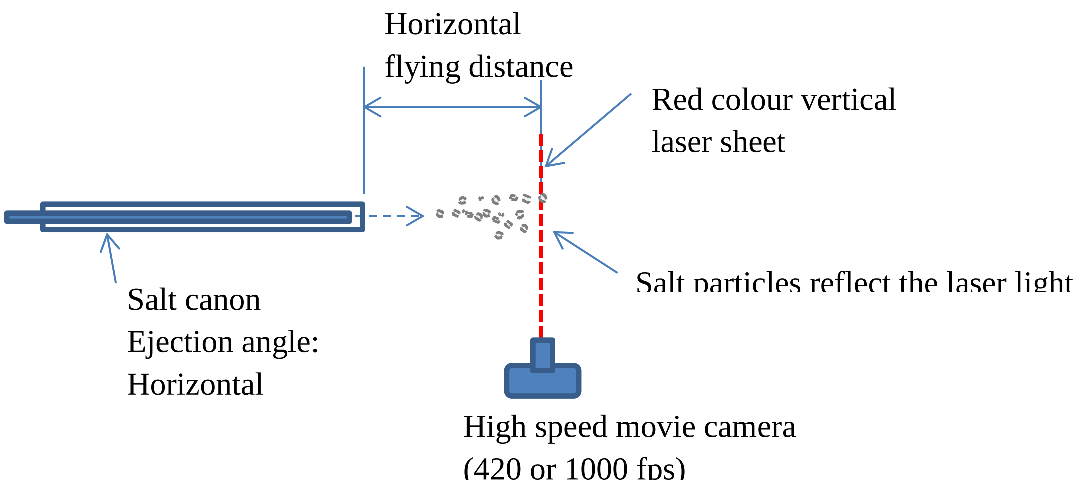

Figure 10: Salt particle reflects red laser light, which enables to capture the moment when the salt-swarm-front passing through the laser sheet on the high speed movie.

air transportation. So, the landing velocity of about 6 m s^{-1} is lesser than what found during real salt spreading.

Particles impacted with the surface at a landing angle of about 15° did not bounce backwards. A thin water layer on the surface reduced particle bouncing, but the effect was dependent on the kinetic energy of the particle. A large particle broke through the water layer and bounced on the surface while smaller particles landed on the water surface without bouncing.

It was observed that a salt particle in air spins due to air resistance acting on at the irregular shaped surface parts, i.e. the spin is caused by aerodynamic effects. Furthermore, high speed movies showed that impact with surface also can cause high speed spinning, i.e. this type of spin is caused by the mechanical impact. As the mechanisms of these two phenomena are different, the nature and effects of them on the particle trajectory might also differ.

High speed movies showing these phenomena can be downloaded from the following links.

- Free-falling large salt particles bouncing on dry roofing felt: Landing velocity = ca. 3 m s^{-1}, 420 fps
  https://www.dropbox.com/s/re1j8rwa4eyh1yv/C%204823%20Free%20drop%20onto%20roofing%20felt%20Dry%20B%20-%20Copy.mp4?dl=0

  Free-falling large salt particles bouncing on wet roofing felt: Landing velocity = ca. 3 m s^{-1}, 420 fps
  https://www.dropbox.com/s/4m8hu20kgt6xr96/D%204830%20free%20drop%20onto%20roofing%20felt%20wet%20B%20-%20Copy.mp4?dl=0

- Large salt particles bouncing on dry roofing felt: Landing velocity = ca. 6 m s^{-1}, Landing angle = ca. 15°, 210 fps.
  X-Z plane:
  https://www.dropbox.com/s/hmy4kq0jo9uevot/E%204874%20rock%20salt%20large%20particle%2015%20deg%20210%20fps%20dry%20B%20-%20Copy.mp4?dl=0
  X-Y plane
  https://www.dropbox.com/s/gsif3hbof67szro/F%204884%20rock%20salt%20large%20particle%2015%20deg%20210%20fps%20XY%20plane%20dry%20B.mp4?dl=0

- Large salt particles bouncing on wet roofing felt: Landing velocity = ca. 6 m s^{-1}, Landing angle = ca. 15°, 210 fps.
  X-Z plane:
  https://www.dropbox.com/s/3ee96a81870q68c/G%204976%20rock%20salt%20210%20fps%20wet%20B.mp4?dl=0
  X-Y plane:
  https://www.dropbox.com/s/962jwna89md37hh/H%204978%20rock%20salt%20210%20fps%20XY%20plane%20wet%20B.mp4?dl=0

- Small salt particles (vacuum salt) tend to stick on the surface: Landing velocity = ca. 6 m s^{-1}, Landing angle = ca. 15°, 210 fps.
  X-Z plane

https://www.dropbox.com/s/t51obd6pickhvve/I%204877%20table%20salt%2015%20deg%20210%20fps%20dry%20B.mp4?dl=0

X-Y plane
https://www.dropbox.com/s/ccm80235wr5nikf/J%204886%20table%20salt%2015%20deg%20210%20fps%20XY%20plane%20B.mp4?dl=0

Discussion

The purpose of the reported studies was to determine some key parameters for the software. It covers visual observation of particle motion, shape and mass of particles and bouncing behaviour on different materials. In order to develop the 3-S simulation software a number of other parameters need to be determined. These include but are not restricted to determination of air resistance coefficient for salt particles and coefficient of restitution with road surface with different materials and structures. Studies are needed on the mechanism behind the spin of salt particles and its effects on particle trajectory and on effects of swarm-transport of salt particles on salt distribution on the road. The swarm-transport subject is particularly important when dealing with the spreading of small particles.

The present study was focused on dry rock salt and vacuum salt. Further studies are needed to extend the software to cover wetted salt and salt brine.

Conclusions

A light sensitive high speed camera with a frame rate up to 1000 fps is useable for recording of salt particle motions. For indoor testing halogen lamps or fluorescent lamp can be used. However, whenever possible natural sun light should be used. The red laser was useful to enhance the recognition of the moving white salt particles.

Free falling velocities of salt particles of 10 to 100 mg achieved a velocity of around 3 m s^{-1} when they fell 0.4m. The rock salt can be considered as random shaped. This means that salt particles are going to be implemented as perfect spheres in the deterministic approach of the 3-S software.

Particles impacted with the surface at a landing angle of about 15^{o} did not bounce backwards. It was noticed that small salt particles (vacuum salt) tend to be sticking to the surface after the impact. A thin water layer on the surface reduced the particle bouncing. The bouncing was highly influenced by the kinetic energy of the particle meaning that a large particle was not so much affected by the water layer. It was also observed that even bouncing on polished surfaces can cause spinning of particles that might result in unpredictable motion.

References

Hisamitsu Takai, 2012a: Standardisation of test method for salt spreader, Air flow experiments. **Report 8**: Observation of salt particle trajectory from spreader disc to road surface. Aarhus University, Engineering Centre Bygholm, Test and Development.

http://pure.au.dk/portal/da/publications/observation-of-salt-particle-trajectory-from-spreader-disc-to-road-surface(bec50ee9-866a-44b3-97e8-a9c93326995b).html

Hisamitsu Takai, 2012b: Standardisation of test method for salt spreader, Air flow experiments. **Report 10:** Simulation of salt particle trajectory from spreader disc to road surface, Aarhus University, Engineering Centre Bygholm, Test and Development. http://pure.au.dk/portal/da/publications/simulation-of-salt-particle-trajectory-from-spreader-disc-to-road-surface(be325da2-a8ab-4cc0-9422-4844026c8c8f).html